

Mild Benzene-Thermal Route to GaP Nanorods and Nanospheres

Shanmin Gao,^{†,‡} Yi Xie,^{*,†} Jun Lu,[†] Guoan Du,[†] Wei He,[†] Deliang Cui,[§] Baibiao Huang,[§] and Minhua Jiang[§]

Structure Research Laboratory, University of Science and Technology of China, Hefei, Anhui 230026, PRC, Scientific Research Institute of Shandong Ocean Chemical Industry, Shouguang, Shandong 262737, PRC, and National Key Laboratory of Crystal Materials, Institute of Crystal Materials, Shandong University, Jinan, Shandong 250100, PRC

Received April 24, 2001

GaP nanorods and nanospheres were synthesized from a mild benzene-thermal route at 240 and 300 °C, respectively, using Na, P, and GaCl₃ as the starting materials. The structure of the products was identified as zinc blende phase by X-ray powder diffraction (XRD). Transmission electron microscopy (TEM) images showed that, when the reaction temperature was 240 °C, the products were nanorods with widths of 20–40 nm and lengths of 200–500 nm and nanospheres with diameters of 20–40 nm. However, when the reaction temperature was increased to 300 °C, the products were only nanospheres, and the diameters increased to 40–60 nm. The reaction proceeded through a metallic gallium intermediate, and a solution–liquid–solid (SLS) mechanism was proposed for the one-dimensional growth. The products were also investigated by UV–vis absorption and X-ray photoelectron spectroscopy.

Introduction

The dependence of physical properties of materials on grain size is a well-known phenomenon. Because the nanometer semiconductor quantum dots exhibit optical and electronic properties from their corresponding bulk semiconductor materials, some of the current research in the materials processing field has focused on the design and synthesis of compound semiconductor nanometer materials. The quantum confinement effects are the basis of new and unusual molecular electronic devices.¹ Current directions in this field of research include the different new appropriate preparation techniques of semiconductor nanoparticles and the modifications of quantum particles by means of surface chemistry,² but most studies in this field have focused on II–VI semiconductor nanocrystals, such as CdS and CdSe.^{3–6}

The techniques of chemical synthesis and theoretical calculation of them have been developed greatly.^{7–11}

Recently, several experimental techniques have been developed for the preparation of III–V nanocrystalline semiconductor compounds. Wells and co-workers reported the reaction of InX₃ (X = Cl, Br, I) with As(SiMe₃)₃ and P(SiMe₃)₃ to synthesize InAs and InP nanocrystalline by heating the products, respectively.¹² Micic et al. synthesized nanocrystalline InP by using P(SiMe₃)₃ and other organometallics in a solution of trioctylphosphine oxide at 270 °C for several days.¹³ Lian Butter and co-workers confined GaAs nanocrystals by refluxing GaCl₃ with As(SiMe₃)₃ in decane at 180 °C for 72 h.¹⁴ In addition, there are other routes, such as solve-thermal reaction¹⁵ and pyrolysis of single-source

* To whom correspondence should be addressed. E-mail: yxie@ustc.edu.cn.

[†] University of Science and Technology of China.

[‡] Scientific Research Institute of Shandong Ocean Chemical Industry.

[§] Shandong University.

- Alivisatos, A. P. *Science* **1996**, *271*, 993.
- Spanhel, L.; Anderson, M. A. *J. Am. Chem. Soc.* **1987**, *109*, 5649.
- Murray, C. B.; Norris, D. B.; Bawendi, M. G. *J. Am. Chem. Soc.* **1993**, *115*, 8706.
- Matthew, M.; Vali, H.; Eisenberg, A. *Chem. Mater.* **1998**, *10*, 1021.
- Lin, J.; Cates, E.; Bianconi, P. A. *J. Am. Chem. Soc.* **1994**, *116*, 4738.
- Anderson, M. A.; Gorer, S.; Penner, R. M. *J. Phys. Chem. B* **1997**, *101*, 5895.

- Katari, J. E. B.; Colvin, V. L.; Alivisatos, A. P. *J. Phys. Chem.* **1994**, *98*, 4109.
- Murray, C. D.; Kagan, C. R.; Bawendi, M. G. *Science* **1995**, *270*, 1335.
- Klein, D. L.; Roth, R.; Lin, A. K. L.; Alivisatos, A. P.; Mceuen, P. L. *Nature* **1997**, *389*, 699.
- Dabbousi, B. O.; Bawendi, M. G.; Onitsuka, O.; Rubner, M. F. *Appl. Phys. Lett.* **1995**, *66*, 1316.
- Korgel, B. A.; Monbouquette, H. G. *J. Phys. Chem. B* **1997**, *101*, 5010.
- Wells, R. L.; Aubuchon, S. R.; Kher, S. S.; Lube, M. S.; White, P. S. *Chem. Mater.* **1995**, *7*, 793.
- Micic, O. I.; Curitis, C. J.; Jones, R. M.; Sprague, J. R.; Nozik, A. J. *J. Phys. Chem.* **1994**, *98*, 4966.
- Butler, L.; Redmond, G.; Fitzmaurice, D. *J. Phys. Chem.* **1993**, *97*, 10750.

precursors,¹⁶ to synthesize III–V compound nanocrystallines, and each of these techniques has advantages and disadvantages. The properties and theoretical calculation of these compound nanocrystallines were also studied. For example, the spectroscopic behavior of colloidal InP quantum dots has been investigated as a function of quantum dot diameter¹⁷ and the electronic structure, surface effect, and red-shifted emission.¹⁸ The theory of size-dependent resonance Raman intensities in InP nanocrystals¹⁹ and optical properties of GaAs nanocrystals²⁰ were also studied, but most of the studies have focused on InP, InAs, and GaAs, with respect to GaP nanocrystals, while there are relatively fewer studies of their syntheses and properties.

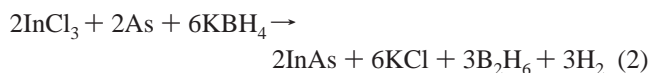
The most important way to prepare GaP is the metal–organic route. Dougall and co-workers²¹ have reported that GaP semiconductor clusters can be synthesized in zeolite by using the reaction $(\text{Me}_3)\text{Ga} + \text{PH}_3 \rightarrow 3\text{CH}_4 + \text{GaP}$. At refluxing temperature, GaP nanocrystallines were obtained from GaCl_3 and $\text{P}(\text{SiMe}_3)_3$ or $(\text{Na/K})_3\text{P}$ and GaX_3 in toluene or other solvent,^{22,23} respectively. Another important method for preparing GaP is the solid-state metathesis, in which GaX_3 ($\text{X} = \text{F}, \text{Cl}, \text{I}$) and Na_3P are used as the raw materials,^{24,25} but this process requires an extra washing step to remove starting materials and byproducts.

Very recently, a lot of work on the preparation of one-dimensional structures, such as nanowires or nanowhiskers, has been done, and important progress has been made. Nanotubes and nanowires exhibit a wide range of electrical and optical properties, which depend sensitively on their sizes and shapes.^{26–31} Buhro and co-workers have reported a solution–liquid–solid (SLS) mechanism for the growth of InP, InAs, and GaAs nanofibers,^{32–34} which is closely

analogous to the well-known vapor–liquid–solid (VLS) mechanism.³⁵ The reaction employed in the SLS growth is described in eq 1.



Our group reported another solution phase method for the synthesis of InAs nanofibers at low temperature.³⁶ The route is described in eq 2.



The preparation of III–V compound semiconductor materials is an arduous task, because toxic and dangerous precursor materials are usually used. The use of EH_3 in eq 1 is of particular concern because of its carcinogenic and mutagenic properties. Equation 2 is a safer route, and the further advantage of this route is that the reactants are available, but the products contain H_2 and B_2H_6 , which increase the danger of the reaction process. As to the previous work, the synthesis of one-dimensional III–V compound semiconductors almost always focused on InP, InAs, GaAs, and GaN,^{37,38} and we have never seen the special topic of the synthesis of GaP nanorods. In this paper, we exploit another route to prepare GaP nanorods and nanospheres. Taking the toxicity of phosphorus into account, we selected red phosphorus as the phosphorus feedstock in the present process. If white phosphorus was used as the phosphorus source, a warning on the possibility of sparking in air should be noticed; furthermore, a more extensive warning on its toxicity is needed.

Experimental Section

A. Synthesis of GaP Nanorods and Nanospheres. All analytical grade solvents used in our experiments were dried by sodium chips and distilled in flowing nitrogen gas. Reactions were carried out in a Teflon-lined autoclave. A 0.68 g (0.03 mol) portion of sodium, 0.309 g (0.01 mol) of red phosphorus, and 1.76 g (0.01 mol) of gallium chloride were mixed in benzene, and then the mixture was added to a Teflon-lined autoclave. Concurrently, benzene was added to raise the filling ratio to ~60–75%. After the air in the solution was expelled by bubbling with nitrogen gas (99.999% pure), the autoclave was sealed and heated to 240 and 300 °C for 6 h, respectively, and then cooled to room temperature naturally. The precipitates were filtered out, in which a few of spherules with metallic sheen were observed. Then, the precipitates were washed with absolute ethanol, 2 M HCl, and distilled water in sequence. Finally, they were dried at 80 °C under vacuum for 5 h. The yield of GaP based on gallium is about 87%.

B. Characterization of the Products. The X-ray diffraction pattern of the dried powders was collected on a D/max- γ A model X-ray diffractometer with Ni-filtered $\text{Cu K}\alpha$ radiation. The X-ray

- (15) Xie, Y.; Qian, Y.; Wang, W.; Zhang, S.; Zhang, Y. *Science* **1996**, *272*, 1926.
 (16) Green, M.; O'Brien, P. *Chem. Commun.* **1998**, 2459.
 (17) Micic, O. I.; Cheong, H. M.; Fu, H. X.; Zanger, A.; Spragus, J. R.; Mascarenhas, A.; Nozik, A. J. *J. Phys. Chem. B* **1997**, *101*, 4904.
 (18) Fu, H. X.; Zanger, A. *Phys. Rev. B* **1997**, *56*, 1496.
 (19) Shiang, J. J.; Wolter, R. H.; Heath, J. R. *J. Chem. Phys.* **1997**, *106*, 8981.
 (20) Uchida, H.; Curtic, C. J.; Kamat, P. V.; Jones, K. M.; Nozik, A. J. *J. Phys. Chem.* **1992**, *96*, 1156.
 (21) Dougall, J. E. M.; Eckert, H.; Stucky, G. D.; Herron, N.; Wang, Y.; Moller, K.; Bein, T. *J. Am. Chem. Soc.* **1989**, *111*, 8006.
 (22) Aubuchon, S. R.; Mcphail, A. T.; Wells, R. L.; Giambra, J. A.; Bowser, J. K. *Chem. Mater.* **1994**, *6*, 82.
 (23) Kher, S. S.; Wels, R. L. *Mater. Res. Soc. Symp. Proc.* **1994**, *351*, 293.
 (24) Treece, R. E.; Macala, G. S.; Rao, L.; Franke, D.; Eckert, H.; Kaner, R. B. *Inorg. Chem.* **1993**, *32*, 2745.
 (25) Treece, R. E.; Macala, G. S.; Kaner, B. R. *Chem. Mater.* **1992**, *4*, 9.
 (26) Yan, P.; Xie, Y.; Qian, Y.; Liu, X. *Chem. Commun.* **1999**, 1293.
 (27) Xie, Y.; Yan, P.; Lu, J.; Qian, Y.; Zhang, X. *Chem. Commun.* **1999**, 1969.
 (28) Kaber, J. A.; Gibbons, P. C.; Buhro, W. E. *J. Am. Chem. Soc.* **1997**, *119*, 5455.
 (29) Duan, X. F.; Lieber, C. M. *J. Am. Chem. Soc.* **2000**, *122*, 188.
 (30) Gudiksen, M. S.; Lieber, C. M. *J. Am. Chem. Soc.* **2000**, *122*, 8801.
 (31) Su, H.; Xie, Y.; Gao, P.; Lu, H.; Xiong, Y.; Qian, Y. *Chem. Lett.* **2000**, 790.
 (32) Trentler, T. J.; Hickman, K. M.; Geol, S. C.; Viano, A. M.; Gibbons, P. C.; Buhro, W. E. *Science* **1995**, *270*, 1791.
 (33) Trentler, T. J.; Goel, S. C.; Hickman, K. M.; Viano, A. M.; Chiang, M. Y.; Beatty, A. M.; Gibbons, P. C.; Buhro, W. E. *J. Am. Chem. Soc.* **1997**, *119*, 2172.
 (34) Buhro, W. E.; Hickman, K. M.; Trentler, T. J. *Adv. Mater.* **1996**, *8*, 685.

- (35) Wagner, R. S. In *Whisker Technology*; Levitt, A. P., Ed.; Wiley: New York, 1970, chapter 3.
 (36) Xie, Y.; Yan, P.; Lu, J.; Wang, W.; Qian, Y. *Chem. Mater.* **1999**, *11*, 2619.
 (37) Han, H.; Fan, S.; Li, Q.; Hu, Y. *Science* **1997**, *277*, 1287.
 (38) Morales, A.; Lieber, C. M. *Science* **1998**, *279*, 208.

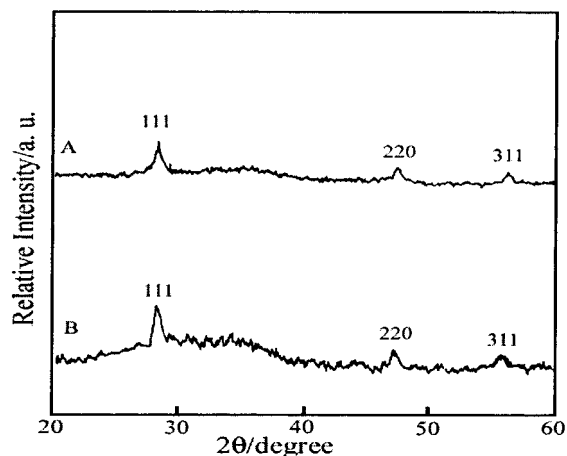


Figure 1. XRD pattern of the samples obtained by reacting 6 h at (A) 240 °C and (B) 300 °C.

beam voltage was 45 kV, and the beam current was 40 mA. The optical absorption spectra were collected at room temperature with a Hitachi 340 UV–vis–NIR recording spectrophotometer with 1 cm quartz cuvettes. The powders were milled and ultrasonically dispersed in benzene. A blank solution of benzene was used as the reference. Transmission electron microscopy (TEM) images of the samples were obtained with a Hitachi model H800 transmission electron microscope, using an accelerating voltage of 150 kV. Samples were deposited from benzene solutions of the products onto thin amorphous carbon films supported by copper grids. X-ray photoelectron spectra (XPS) were recorded on an ESCALab MKII instrument with Mg K α radiation as the exciting source. The binding energies obtained in the XPS analysis were corrected by referencing the C 1s peak to 284.60 eV.

Results and Discussion

Reaction of GaCl₃, sodium, and red phosphorus at 240 and 300 °C in benzene yielded a fine gray-black powder. Figure 1 shows the X-ray diffraction patterns of the GaP powders. Pattern A is the sample which reacted at 240 °C, and pattern (B) is the sample which reacted at 300 °C. The peaks correspond to the (111), (220), and (311) planes of GaP with a zinc blende structure, respectively. Broadening of the peaks is due to the decreasing particle size. According to the Scherrer equation, it could be estimated that the average particle sizes are about 32 nm for A and 36 nm for B. TEM images for the sample prepared at 240 °C show nanorods with diameters of 20–40 nm and lengths of 200–500 nm and nanospheres with diameters of 20–40 nm (Figure 2A). Selected area diffraction within a linear segment of a rod (marked with an arrow) gives single-crystal patterns, which could be indexed for the [134] zone axis of crystalline GaP and suggests that the rod axis was the [111] direction (Figure 2B). Rods of cubic compounds (such as III–V semiconductors)^{32–34} and elements (such as Si)³⁸ obtained from VLS and SLS processes typically grow along the [111] direction. Only nanospheres with an average diameter of 40 nm were clearly seen for the sample prepared at 300 °C (Figure 2C). Figure 2D is the electron diffraction pattern of sample B. The diffraction rings illustrate the existence of some amorphous composition in the product, which is in accordance with the XRD pattern (Figure 1B).

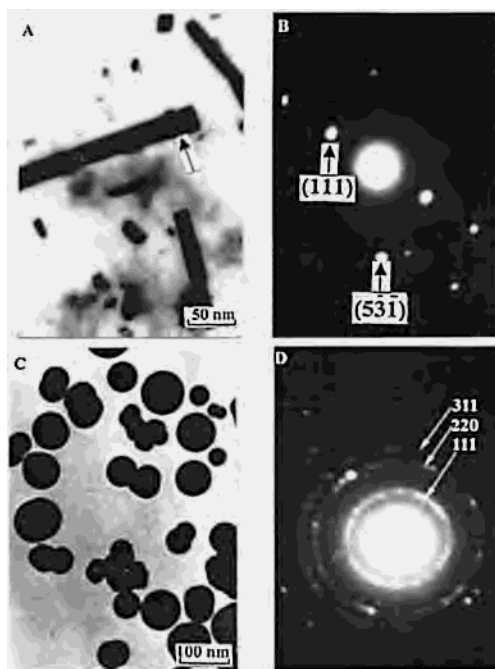


Figure 2. (A) TEM image for GaP nanorods prepared at 240 °C. (B) Selected area electron diffraction pattern for GaP nanorods. (C) TEM image for GaP nanospheres at 300 °C. (D) Selected area electron diffraction pattern for GaP nanospheres.

Among the three well-known whisker-growth mechanisms, that is, vapor–liquid–solid (VLS), vapor–solid (VS), and solution–liquid–solid (SLS), the SLS mechanism is most likely to function under the present conditions because both cases involved reactions in organic solvent, and in both cases, gallium coexisted with the products. In this system, gallium atoms easily form from the reduction of GaCl₃ by sodium. The newly reduced gallium atoms are active enough to react with phosphorus immediately. However, if the surrounding phosphorus is insufficient, the reduced gallium atoms will aggregate into spherules because of its very low melting point (302.65 K) and coexist with the final products. The molten gallium can presumably be regarded as the intermediate phase in the process of preparing GaP nanocrystals. When the precipitate is filtered, a few spherules with metallic sheen can be observed, and its XRD patterns indicated that these spherules were metallic gallium, supporting the idea that molten gallium is an intermediate in the growth process of GaP nanocrystals. In addition, if benzene and water in the filtered solution were vaporized, a white solid substance appeared, which is NaCl, as proved by its XRD patterns. These two facts further confirmed the proposed mechanism of rod growth. According to the SLS mechanism, the reaction should be



So, when the reactions were carried out at 240 °C, the products were GaP nanorods, but an interesting phenomenon was discovered: there were some nanospheres coexisting in the products prepared at 240 °C and only nanospheres in

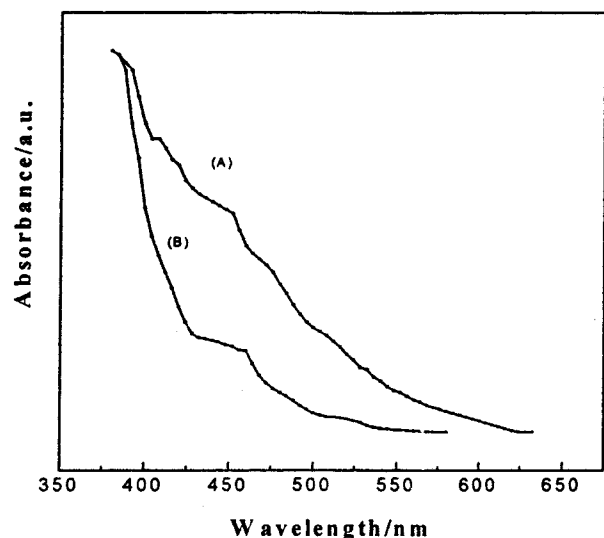


Figure 3. Optical absorption spectra of samples prepared at (A) 240 °C and (B) 300 °C.

the products prepared at 300 °C. The similar phenomenon has been observed previously.³⁶ However, there has been no suitable explanation for this phenomenon in the previous work. Here, we propose a reasonable explanation for it as follows. It is well-known that the physical properties of materials, such as the melting point, depend sensitively on the particle size. The melting point of nanocrystals falls quickly with decreasing particle size. For example, the melting point of Pb bulk material, which is 600 K, falls to 288 K when the particle size decreases to 20 nm. Ag nanocrystals begin to melt when the temperature is lower than 373 K, while the melting point of Ag bulk material is 1173 K. According to these facts, we hypothesize that 300 °C may be the melting point or over the melting point of GaP nanorods at the present size under the current benzene-thermal condition. At this temperature (300 °C), the GaP nanorods may melt and produce GaP nanospheres. That may be why only nanospheres were obtained in the final products prepared at 300 °C. With regard to the nanospheres in the products prepared at 240 °C, the GaP nanorods with smaller size may melt and produce relative GaP nanospheres; meanwhile, GaP nanorods with larger size remain, resulting in the coexistence of larger GaP nanorods and smaller GaP nanospheres in the final product.

Our UV–vis spectroscopic investigations provided insight into the quantum confinement in GaP nanocrystals. Figure 3 shows blue-shifted UV–vis absorption spectra of GaP nanorods prepared at 240 °C and nanospheres prepared at 300 °C dispersed in benzene. Both absorption spectra show long tails near the absorption edge because of defect or particle size distribution. From the absorption spectra, one can clearly see that curve B of the GaP nanospheres has a more obvious shoulder peak and its wavelength region is narrower than curve A of GaP nanorods. This means that GaP nanospheres are perfect in crystal grains and have better uniformity in particle size than GaP nanorods, which grow with high orientation. The result is consistent with those of the TEM images. The particle size giving rise to the

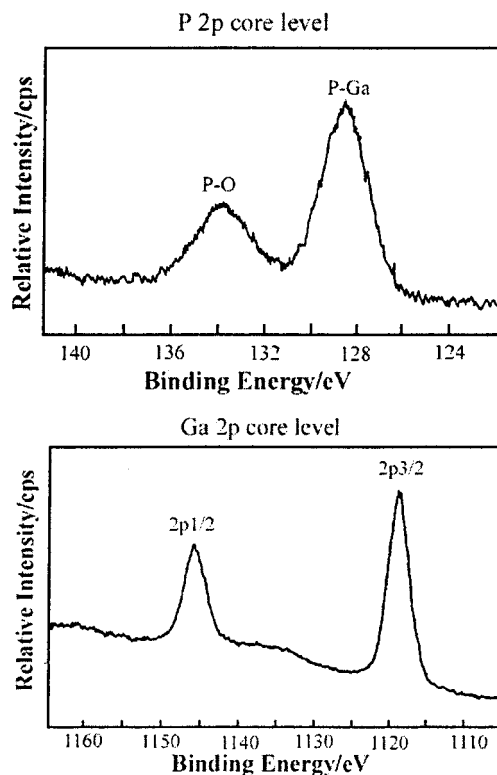


Figure 4. X-ray photoelectron spectra of samples prepared at 240 °C.

absorption onset at 460 nm was estimated to be approximately 32 nm using the effective mass approximation (EMA).

X-ray photoelectron spectra (XPS) analysis was used to measure the elemental composition of the nanocrystals. Higher resolution spectra taken of the Ga 2p region and P 2p region were shown in Figure 4. The gallium core is spin-orbit split to $2p_{3/2}$ and $2p_{1/2}$ with the $2p_{3/2}$ peak at 1117.2 eV, both corresponding to Ga from GaP. The P 2p core shows two peaks, one at 128.5 eV corresponding to P from GaP and the other at 133.2 eV corresponding to oxidized P species. Because of the higher surface areas and reactivity of the nanocrystals, the atoms on the surface are much more easily oxidized when they are exposed to air. Thus, the phosphorus atoms on the surface of the products may turn to oxide phosphorus gradually, resulting in the oxidized phosphorus species in the XPS spectrum. In our previous work for InAs,³⁶ similar phenomena have been reported, and Alivisatos³⁹ et. al have also observed a similar phenomenon in InP nanocrystals. Peak areas of these high-resolution scans were measured and used to calculate the Ga-to-P ratio for the nanocrystals. Quantification, in which only the P 2p peak corresponding to GaP was used, gave a Ga-to-P ratio of 1.09:1. As mentioned previously, there was trace gallium removed by hydrochloric acid, so it is no wonder that more phosphorus atoms than gallium atoms occupied the surface sites of the product. This excess phosphorus is also responsible for the oxidized P 2p peak at 133.2 eV. Thus, we conclude that the nanocrystals are close to stoichiometric.

(39) Guzelian, A. A.; Katari, J. E. B.; Kadavanich, A. V.; Banin, U.; Hamad, K.; Juban, E.; Alivisatos, A. P.; Wolters, R. H.; Arnold, C. C.; Heath, J. R. *J. Phys. Chem.* **1996**, *100*, 7212.

Conclusion

Samples of 20–40 nm × 200–500 nm GaP nanorods and 20–60 nm GaP nanospheres were successfully synthesized via a novel reaction of GaCl₃, P, and Na at 240 and 300 °C under benzene-thermal conditions. The reaction proceeds with gallium as the likely intermediate. The SLS mechanism is likely responsible for the nanorod growth.

Acknowledgment. Financial support from the Chinese National Foundation of Natural Science Research through the Outstanding Youth Science Fund and Huo Yingdong Foundation for Young Teachers is gratefully acknowledged.

IC010431Y